PSFC/JA-97-27

# Measurements of the H-mode Pedestal Region on Alcator C-Mod

A.E. Hubbard, R.L. Boivin, R.S. Granetz, M. Greenwald,
I.H. Hutchinson, J.H. Irby, Y. In, J. Kesner, B. LaBombard,
Y. Lin, J.E. Rice, T.S. Pedersen, J.A. Snipes,
P.C. Stek[1], Y. Takase[2], S.M. Wolfe, S. Wukitch

December 1997

Plasma Science and Fusion Center
Massachusetts Institute of Technology
Cambridge, MA 02139

[1]Present address, Jet Propulsion Laboratory, Pasadena, CA 91109-8099.
[2]Present address, Dept. of Physics, University of Tokyo, Japan.

To be published in Physics of Plasmas.

This work was supported in part by the U. S. Department of Energy Contract No. DE-AC02-78ET51013. Reproduction, translation, publication, use and disposal, in whole or in part by or for the United States government is permitted.

# Measurements of the High Confinement Mode Pedestal Region on Alcator C-Mod

A. E. Hubbard, R. L. Boivin, R. S. Granetz, M. Greenwald, I. H. Hutchinson, J. H. Irby, Y. In, J. Kesner, B. LaBombard, Y. Lin, J. E. Rice, T. Sunn Pedersen, J.A. Snipes, P. C. Stek[a)], Y. Takase[b)], S. M. Wolfe, S. Wukitch

*Plasma Fusion Center, Massachusetts Institute of Technology, Cambridge, Massachusetts 02139*

Measurements of the steep transport barrier at the edge of the Alcator C-Mod tokamak (I. H. Hutchinson *et.al.*, Phys. Plasmas **1**, 1511 (1994)) are presented. The parameters at the top of this barrier are in the range $T_e$=150–750 eV and $n_e = 0.5 - 3.3 \times 10^{20}\,\mathrm{m}^{-3}$, depending on the confinement regime. Type III Edge Localized Modes (ELMs) have an upper temperature limit. $T_e$ pedestal profiles show a barrier width $\Delta_T \simeq$8 mm. Soft x-ray emissivity profiles are narrower, with $\Delta$ =2–4 mm. Edge currents are calculated to alter the ideal stability boundary favourably, leading to ideally stable pedestal profiles. High frequency, broadband, edge density fluctuations are sometimes observed in H-mode and are associated with enhanced particle transport. Coherent magnetic fluctuations localized near the pedestal are also seen.

PACS: 52.55.Fa, 52.25.Fi, 52.70.La, 52.25.Gj

[a)] Present address, Jet Propulsion Lab, Pasadena, CA 91109-8099

[b)] Present address, Department of Physics, University of Tokyo, Japan

## I. INTRODUCTION

An essential feature of the high confinement (H-mode)[1] regime seen on many tokamaks and other toroidal devices is a steepening of density and temperature gradients near the separatrix. This outer region is the first to show confinement changes, which may be followed by less dramatic improvements in the rest of the plasma. It is also in this so-called 'pedestal' region that fluctuations are generally observed to drop at the transition from the usual low confinement (L-mode) to the H-mode. Stabilization of turbulence via $E \times B$ sheared flows in the edge has been proposed as an explanation for this phenomenon[2]. Studying the pedestal region of the plasma is thus critical to understanding both the mechanism of the L-H transition and the confinement improvement which results from it.

The importance of parameters in the pedestal region has been underscored by transport models which predict that the core transport is substantially affected by the boundary conditions in the outer 20% of the plasma. For example, the IFS/PPPL (Institute for Fusion Studies/Princeton Plasma Physics Laboratory) model[3] shows a strong sensitivity of core confinement to edge temperature, due to marginal stability of the ion temperature gradient mode. Results on the Alcator C-Mod tokamak[4] (C-Mod) have shown a good correlation between the edge temperature and the global energy confinement, which holds for both L and H-mode plasmas[5]. The core temperature gradients also increase with edge temperature, consistent with a marginally stable transport situation. It should be noted that while transport theories are mainly sensitive to the ion temperature $T_i$, at the high densities typical of C-Mod electron and ion temperatures are expected to be tightly coupled, especially near the plasma edge.

The pedestal region is less well understood than the core plasma, leading to significant uncertainties in predicting the boundary conditions for future machines. Recently, diagnostic advances have made possible more detailed measurements of the edge transport barrier. DIII-D[6] reports electron pressure widths which scale equally well with $(\rho_{i,pol}/R)^{0.66}$ or with $(\beta_{pol})^{0.4}$, where both the ion poloidal gyroradius $\rho_{i,pol}$ and the edge poloidal beta are calculated at the top of the pedestal[7]. JT-60U[8] reports that the width of the barrier in $T_i$ varies linearly with $\rho_{i,pol}$[9]. On the other hand, recent results from the Axisymetric Divertor Experiment (ASDEX) Upgrade[10] indicate little or no dependence of the width of the barrier in $T_e$ on $\rho_{i,pol}$[11].

H-modes have been observed on Alcator C-Mod($R = 0.67\,\mathrm{m}, a = 0.22\,\mathrm{m}, \kappa \leq 1.8$) at magnetic fields in the range 2.6–7.9 T, plasma currents $I_p$ of 0.6–1.2 MA and at line averaged density $\overline{n}_e$ up to $4.8 \times 10^{20}\,\mathrm{m}^{-3}$. H-modes are either ohmic or heated by up to 3.5 MW of ion cyclotron resonance heating (ICRH)[12]. Lower triangularity is typically 0.5–0.6, while the upper triangularity is 0.3–0.8. The experiments thus cover a unique parameter space, particularly in $B_T$ and density. Measurements on C-Mod aim to help resolve the present uncertainty regarding the relevant variables and scalings which determine both the pedestal height and width.

Many H-modes on Alcator C-Mod are ELM-free, that is they do not exhibit any 'Edge Localized Modes', or ELMs[13]. Type III ELMs are sometimes, but not usually, seen. We have never observed the regular, large, 'Type I' ELMs reported by most other tokamaks at high heating power. An H-mode regime has been found on C-Mod which shows lower particle and impurity confinement than ELM-free H-mode, leading to steady state conditions, while still maintaining good energy confinement[5,12]. These confinement properties are reminiscent of ELMy H-modes on other machines. However, in this regime there are no signatures of discrete ELMs, which elsewhere cause concerns about instantaneous heat flux to the divertor. Rather, the level of edge $D_\alpha$ emission rises steadily, leading to the name 'Enhanced $D_\alpha$' (EDA) H-mode[14]. Understanding this regime is a priority given the potentially attractive features for reactor operation.

Previous analysis of parameters in the outer region of Alcator C-Mod plasmas has concentrated on characterizing conditions just before the L-H and H-L transitions in a variety of core plasma conditions[12,15,16,17,18]. It has been found that, for a given magnetic configuration, a minimum value of edge electron temperature, or its gradient, is required to enter H-mode. The H-L transition occurs at a temperature which is the same as or higher than the L-H threshold; there is thus no favourable hysteresis in this local threshold condition. The threshold $T_e$ shows a strong positive dependence on $B_T$ and a density dependence which can be either flat or weakly negative. When the toroidal field and current were reversed, giving ion $B \times \nabla B$ drifts pointing away from the active lower divertor, both the edge threshold temperature and the global power threshold doubled. Comparisons with theory show that for the favourable drift direction, our measured thresholds are roughly consistent with thresholds in dimensionless ballooning and ion diamagnetic parameters predicted by numerical simulations of turbulence suppression via sheared $E \times B$ flow, carried out

by Rogers and Drake[18,19]. The differences with reversed field are not yet understood, but may imply a role of scrape-off layer (SOL) flows.

This paper will focus on measurements of plasma parameters in the pedestal region during the H-Mode. The diagnostic set used for pedestal measurements on C-Mod will be described in the following section. In section III, the parameters near the top of the transport barrier in the various H-Mode regimes will be presented. Measurements of the structure and width of H-mode pedestals will be shown in Section IV. These enable an analysis of the MHD stability of the pedestal, given in Section V. Conclusions and plans for future studies are given in the final section.

## II. DIAGNOSTICS

Edge studies on C-Mod have concentrated on electron density and temperature since these are the parameters for which the best diagnostic information is available. The primary density profile diagnostic is an interferometer with 10 vertical chords[20]. However, the chords are not located close to the separatrix, so that assumptions must be made about the edge density in the inversion process. A parametrization based on probe measurements of the SOL is used. More detailed information on the edge density and its fluctuations is obtained from reflectometry[21]. Five amplitude-modulated channels operating in the ordinary mode probe density layers between 0.3 and 1.5 $\times 10^{20}\,\mathrm{m}^{-3}$. The absolute calibration of the position of each reflecting layer is estimated at $\pm$ 5 mm. The reflectometer has a time resolution of 0.5 msec for profile measurements. Rapid digitization of the 88 GHz channel has been used for some discharges to monitor changes in the level of density fluctuations at the critical density layer with $\delta t = 2.4\ \mu s$.

Electron temperature profiles on C-Mod are measured by electron cyclotron emission (ECE) spectrometers. For pedestal studies, a nine channel grating polychromator (GPC) is used. This provides $T_e(t)$ at 9 magnetic fields (radii) with instrument-limited frequency resolution giving $\delta R$(FWHM) of typically 9 mm. For the experiments reported here, a digitization rate of 20 kHz was used. Absolute calibration uncertainties are estimated to be $\pm$10%, with lower random noise levels (typically 10 eV). A Thomson scattering system measures at 6 positions with 20 ms time resolution, and generally gives central $T_e$ in good agreement with ECE. However, its spectrometers are not well optimized for the cooler temperatures ($<$ 0.8 keV) typical of the edge pedestal.

Two new diagnostics were added in 1997 specifically to provide higher radial resolution in

the pedestal region. A 38-chord x-ray array views the edge region of the C-Mod plasma with 1.5 mm radial resolution, and 12 $\mu s$ temporal resolution. A 10 micrometer thick beryllium foil cuts out all photon energies below 600 eV. The chord-integrated data from the edge x-ray array have been inverted to get edge emissivity profiles as a function of time. The edge radiated power emissivity is measured using a silicon AXUV diode array which possesses a very thin dead layer on its surface, allowing a flat response across a wide range in photon energies, at least from 20-4000 eV. The array is composed of 19 channels spanning approximately 4 cm near the separatrix, with 2 mm spatial resolution and a better than 100 $\mu s$ time resolution.

C-Mod also has a full set of scrape-off layer and divertor diagnostics[22]. A scanning Langmuir probe, inserted from the bottom of the vessel well away from the divertor region, can reach close to the separatrix. $n_e$ and $T_e$ profiles are measured with a scan time of 40 ms and $\sim$ 0.5 mm radial resolution. These data are important since we find that the transport barrier extends a small distance into the SOL.

To aid in comparison of the different diagnostics used, all data are referenced to surfaces of normalized poloidal flux $\psi$. Radii are then mapped to the outer horizontal midplane. Equilibrium reconstruction based on magnetics diagnostics is carried out by the EFIT code[23]. Accuracy in determining the resolution of the last closed flux surface (LCFS) is estimated at $\pm$ 3 mm.

## III. OPERATIONAL SPACE OF EDGE PEDESTAL PARAMETERS

Parameters near the edge of the plasma have been compiled for a large number of H-mode discharges. We generally take the point at $\psi$ =95%, which has been found in detailed profile measurements to be at or slightly inside the top of the pedestal. As discussed above, inverted edge densities from the interferometer have relatively large uncertainties. The derived pedestal density is typically 70% of $\overline{n}_e$ in both L and H-mode, and may underestimate the actual density in H-mode.

Plotting edge temperature vs edge density has been found to be a useful way of characterizing the 'operation space' of different confinement regimes[24]. Figure 1 shows such a plot for over 400 time slices taken from a wide variety of C-Mod discharges with $B_T \simeq$5.3 T and $I_p$=0.8–1.2 MA. Conditions are not necessarily in steady state at the times chosen. As can be seen, a wide space is essentially filled in, with edge densities from 0.4–3 $\times 10^{20}\,\mathrm{m}^{-3}$ and temperatures from 50 to 750 eV. Even higher H-mode pedestal densities, up to $3.3\times 10^{20}\,\mathrm{m}^{-3}$, have been achieved. However, ECE

emission at the frequency of interest for this field is cut off at 3.1 $\times 10^{20}\,\mathrm{m}^{-3}$ so that edge $T_e$ is no longer measured. While there is some overlap, the different regimes do tend to separate in this space. As was found in threshold studies, L-mode points have $T_e(\psi = 0.95) < 150$ eV, with the exception of a few discharges below our low density limit for H-mode, $\overline{n}_e \simeq 0.7 - 0.9 \times 10^{20}\,\mathrm{m}^{-3}$.

Type III ELMs occur when the pedestal temperature is only slightly above the L-H threshold, up to 200 eV. They are identified by transient increases in $D_\alpha$ and by MHD signatures including high m and n precursors[16]. Above this temperature, which does not show a density dependence, ELMs consistently disappear, suggesting stabilization of the responsible mode. The existence of an upper temperature for Type III ELMs has been seen elsewhere[7,24] and has been suggested as evidence that these ELMs are due to a resistive instability[13]. Measurements of the threshold on different machines can help to distinguish between possible models. A scaling for stabilization of a flute dissipative instability predicted ELMs would be seen up to 500 eV at this field on C-Mod[25], which disagrees with our observations. Operationally, Type III ELMs tend to occur either for discharges with input power not far above the L-H threshold or in cases with high radiated power, which cools the edge. In high power, well conditioned discharges the pedestal temperature quickly rises above 200 eV and at most a few ELMs are seen.

Most C-Mod discharges remain ELM-free for nearly the whole duration of the H-mode. After the initial rise in pedestal temperature and density, the core density typically continues to rise throughout the ELM-free phase. The increases in density and in impurity radiation, due to greatly increased particle and impurity confinement[26], eventually cause the pedestal temperature and confinement to drop. The ELM-free regime has given the highest pedestal temperatures, up to 750 eV, and correspondingly the best confinement enhancement factor, $H_{\mathrm{ITER89-P}}$ (or simply the 'H factor') up to 2.5. This is defined as the ratio of the observed confinement time to that predicted by the ITER89-P L-mode scaling law[27]. Its main operational disadvantage is that conditions are not steady state. As seen in Figure 1, there is a wide variation in $T_{edge}$ in ELM-free discharges even for nominally similar conditions. It tends to decrease with higher radiated power fraction, as might be expected. The correlation of $T_{edge}$ with net conducted power is, surprisingly, not as strong.

The Enhanced $D_\alpha$ regime has pedestal temperatures which typically are more modest than the best ELM-free cases, but can still be up to 650 eV. Average energy confinement is also reduced

by ~10%, with H-factors of 1.5–2.3. This loss is offset by the considerable decrease in particle and impurity confinement, which enables steady state conditions to be maintained with a moderate level of radiation ($P_{rad}/P_{in} \sim 30\%$). While there are typically no signatures of discrete ELMs, high frequency density and sometimes magnetic fluctuations are seen to increase[28]. These will be described in more detail later. From the edge operational space plot, it can be seen that while EDA H-modes tend to occur at high densities [$n_e(\psi = 0.95) \geq 1.5 \times 10^{20}\,\mathrm{m}^{-3}$], the edge parameters overlap those of the ELM-free discharges. This makes it unlikely that the EDA is simply a manifestation of a pressure limit similar to that seen for Type I ELMs[7,11]. The regime persists at temperatures well above those characteristic of L-Mode or Type III ELMs.

The edge density and temperature for plasmas with $B_T = 8$ T, shown in Figure 2, exhibit a similar separation of regimes to that found at 5.3 T. Fewer experiments to date have been run at this field, which uses a D($He^3$) ICRF heating scenario having lower single pass absorption than the D(H) scheme used at 5.3 T. The power threshold increases with $B_T$, so that H-mode can be obtained over a more limited density range and most discharges had power close to the threshold. Pressures are probably limited by the available input power. Higher edge temperatures are seen in L-mode, reflecting the higher local transition threshold. Type III ELMs also occur at higher temperature, up to 350 eV. Most 8 T H-modes are ELM-free, but a few discharges with weakly enhanced $D_\alpha$ have been observed.

## IV. MEASUREMENTS OF PEDESTAL WIDTH

Detailed measurements of the H-mode pedestal region are available for a more limited set of discharges. The density at the plasma edge is seen by the reflectometer to rise very rapidly at the transition. Fig. 3 shows profiles 10 ms before and after a transition from L-mode to ELM-free H-mode. Thomson scattering data, also shown, indicate little change in the core density during this early period. All of the reflectometer channels move close to the separatrix in H-mode, their separation less than the absolute position uncertainty of 1 cm. In fully developed H-modes, the top of the density pedestal typically exceeds the maximum cutoff density of the reflectometer and only the lower part of the pedestal can be covered. In this outer region the density fluctuations drop dramatically at the transition from L-mode to an ELM-free H-mode. At the transition to the EDA regime, in all cases where sufficiently fast data are available, broadband density fluctuations in the

range 50–200 kHz start to increase simultaneous with the rise in $D_\alpha$ emission[28]. This suggests that these fluctuations may be associated with the increased particle transport. The fluctuation spectrum often, but not always, has a peak at $\sim$ 50–140 kHz.

Langmuir probe data show that electron density profiles, as well as temperature profiles, steepen just outside the separatrix. Figure 4 shows profiles taken in two similar 800 kA, 5.3 T discharges. One is just before an L-H transition, and the other late in an ELM-free H-mode. Both $n_e$ and $T_e$ drop outside the separatrix and start to increase about 1 mm from the separatrix. Scale lengths $L_T = T_e/\nabla T_e$ and $L_n = n_e/\nabla n_e$ both decrease from 5 mm to 2 mm, and the apparent transport barrier extends several mm into the scrape-off layer. Further details of SOL transport on C-Mod have been reported previously[22].

The pedestal in $T_e$ is less than the channel separation of the GPC ($\sim$ 2 cm), so that in normal operation details of the pedestal cannot be resolved. A technique of sweeping the toroidal field by 2–3 % has been used to move the radial positions of the channels across the pedestal during a discharge. This had no discernable impact on the plasma behaviour or RF coupling, whereas sweeping the plasma position would significantly perturb the discharge. The $B_T$ ramp takes $\sim$ 80 ms, so the technique is best suited to steady state regimes. Figure 5 shows an example from a 5.3 T, 800 kA EDA H-mode discharge with $\overline{n}_e = 2.7 \times 10^{20}\,\mathrm{m}^{-3}$ and $P_{RF} = 2.4$ MW. The pedestal in this case is 425 eV and has a well defined steep gradient region. The temperature at $R_{LCFS}$ agrees well with an estimate of 125 eV based on parallel heat conduction in the SOL, and shows no evidence of non-thermal emission. The radiation temperature of 60 eV seen well outside the separatrix is due to first harmonic emission (expected for $R - R_{LCFS} > 1$ cm) and possibly to a small spurious response to higher diffraction orders in the grating polychromator.

In order to determine the pedestal width, the measured ECE profile is fit by a *tanh* function as suggested by the DIII-D group[29], defined as $T(R) = A\{tanh[(R_{ped} - R)/\delta] + 1\} + T_{out}$, where $R_{ped}$ is the location of the pedestal midpoint, $\delta = \Delta/2$ is the half-width of the pedestal and $T_{out}$ is the observed offset. For $R < (R_{ped} - \delta)$, a linear term $C(R_{ped} - \delta - R)$ is added. This gives a good fit to the ECE data and results in a full width $\Delta$=12 mm (dashed curve). While sweeping the channel position gives a large number of measurement points, the emission at each time is still subject to the instrumental radial resolution (FWHM=9 mm). Deconvolving the instrument

function gives a narrower actual pedestal width $\Delta_T = 8$mm (solid curve). The maximum gradient is 40 keV/m, as compared to 8 keV/m further inside the plasma. Since this width is comparable to the resolution, it is considered an upper bound.

The pedestal width on C-Mod is clearly narrower than on other tokamaks, making measurements in this region more challenging. For comparison, pedestal widths of $\sim$ 3–6 cm are reported on JET[30,31], 0.7–2 cm on DIII-D[7], 2–2.6 cm on ASDEX Upgrade[11] and 2-7 cm on JT-60U[9]. The higher resolution of the new x-ray and AXUV arrays is thus needed to characterize this region. The power emissivity measured by the AXUV array, similar to the profiles measured by probes, drops outside the separatrix at the L-H transition and increases steeply inside it, as shown in Figure 6. The scale length $\varepsilon/(d\varepsilon/dR)$ decreases from $\sim$15 mm to 4 mm. The high resolution profile extends 1 cm inside the separatrix, and does not show any decrease in slope which would indicate the top of a transport barrier. Emissivity is a function of temperature and impurity density as as well as $n_e$, and lower resolution bolometry and XUV diode measurements show that radiated power peaks at r/a $\sim$ 0.85 during H-mode, dropping in the core. A pedestal structure corresponding to that in $T_e(R)$ or $n_e(R)$ is thus not expected.

The edge x-ray emissivity, in contrast, does show a very clear pedestal which develops at the L-H transition. The peak emissivity rises from 4 kW/m$^3$ to 26 kW/m$^3$ for the same discharge shown in Figure 6, and up to 60 kW/m$^3$ in some cases. The inverted emission profiles, shown in Fig. 7, increase over only 2 radial points, which have a separation of 1.7 mm, and the apparent position of this pedestal is 1 cm inside the separatrix. A *tanh* fit gives widths $\Delta_\varepsilon$ of 3 to 4 mm, varying slightly with time. Widths as small as 2 mm have been measured on some similar discharges.

The interpretation of the x-ray emissivity in terms of plasma temperature and density is unfortunately not straightforward. Bremsstrahlung and recombination of low Z impurities can account for only $\sim$5 kW/m$^3$ under these conditions. A substantial fraction may thus be due to impurity line emission, which can be a strong function of temperature. However, spectrally resolved x-ray measurements in the range 3.7-4.0 Å show no evidence of lines from species such as Ar or Mo near the edge. Spectra at lower energies will be required in order to identify the x-ray sources. The x-ray filter function has decreasing transmission for energies typical of pedestal temperatures. For these reasons, the pedestal in emissivity will tend to be narrower than the $T_e$ or $n_e$ pedestals

and at a position shifted in the direction of hotter plasmas.

An empirical fit, comparing the time behaviour of the peak emission to that of the pedestal temperature and density, shows that the emissivity is well approximated by $\varepsilon = n_e^2 \exp(T_e/T_1)$, where $T_1 \simeq 100$ eV. Applying this function to the radial profiles, and assuming that $T_e$ and $n_e$ have *tanh* profiles with the same width and position (which is not certain), one can model the emission which would result from different profiles. We find that the x-ray pedestal would have a width $\Delta_\varepsilon$ which is 30% narrower and is shifted inward by $\Delta_T/2$. The measured emission would then be consistent with an actual pedestal width of $\simeq$ 5 mm. Analysis of other discharges gives a range of 3-6 mm. This interpretation places a lower bound on the pedestal width for ELM-free H-Modes on C-Mod ($B_T$=5.4 T), but is considered preliminary pending a more complete identification and modelling of the sources of x-ray emission.

## V. MHD STABILITY

Details of the pedestal profiles are critical to assessing the MHD stability of various modes near the plasma edge. As can be seen from the operational space diagram, C-Mod H-modes have a wide range of pedestal parameters. MHD analysis has therefore concentrated on the discharges closest to the constant pressure line shown in Figure 1, which are expected to be most unstable. Since we do not yet have high resolution measurements for the discharges with the highest pedestals, the width measurements given in section IV have been used to estimate the edge pressure gradients.

Figure 8 shows the ideal ballooning stability analysis for a 5.4 T, 1 MA Enhanced $D_\alpha$ H-mode plasma. The discharge has an edge temperature similar to the one shown in Figure 5, but has higher ICRF power (3.5 MW), and density ($\overline{n}_e = 3.8 \times 10^{20}\,\mathrm{m}^{-3}$), and therefore higher pressure. The pressure gradient $P' = dP/d\psi$ is calculated using the experimental $T_e$ and $n_e$ values at R = 0.86 m, and assuming a shape similar to the *tanh* function with $\Delta$ = 8 mm measured for $T_e$(R). $T_i(R)$ is derived using the central $T_i$ measured by neutron diagnostics and adjusting $T_i/T_e$ according to the computed electron-ion equilibration rate at each radius. For this discharge $T_i(0) \simeq 0.9\,T_e(0)$, and $T_i$ is very close to $T_e$ at the edge. $T_i$ profiles derived using this method agree well with high resolution x-ray spectroscopy data in cases when these are available. The maximum total pressure gradient $dP/dR = 5.9 \times 10^6$ Pa/m near the separatrix, which corresponds to $P' = 7.5 \times 10^6$ Pa/Wb/rad in flux coordinates. This kinetic pressure profile is self-consistently included in the equilibrium

reconstruction carried out by EFIT, which is then analysed by the BALOO code[32]. The resulting ideal stability boundary $P'_{crit}$, shown by the thick solid curve, starts to increase at $\psi > 0.95$, the region of steep gradient. This is due to an increase in the deduced edge current, which is consistent with calculated bootstrap current and which significantly modifies the shear profile. A small region of 'second stable access' appears for $\psi > 0.98$. The pressure profile in this case is found to be stable everywhere. In order to illustrate the effect of the edge gradient, the dotted curve shows the stability boundary calculated assuming that there is no pressure pedestal, simply extrapolating the core pressure gradient to the edge and hence avoiding the edge bootstrap current. In this case $|P'_{crit}|$ decreases slightly towards the edge and the 'second stable access' disappears. Qualitatively similar stability results have been reported for parameters typical of DIII-D discharges[32].

Given the proximity to the ideal limit, one might expect that pressure profiles would need to be only 30% narrower in order to exceed the stability limit. However, if steeper gradients are assumed in the reconstruction the stability boundaries shift, in a favorable direction, as the edge current also increases. The edge profiles remain ideal ballooning stable for $P'$ up to $1.4 \times 10^7$ Pa/Wb/rad, which is equivalent in maximum gradient to a pedestal width of $\Delta \sim 4$ mm. This marginal case, which would be consistent with the width estimated from x-ray data, is shown by the dashed curves in Fig. 8. Cases with even higher gradients do become unstable. Ideal stability is consistent with the lack of type I ELMs in C-Mod operation to date. The available RF input power on C-Mod will be doubled to 7 MW in 1998, and it will be of interest to learn to what extent pedestal pressures can be increased before encountering an MHD limit. It is clear that stability calculations are sensitive to details of temperature and density profiles which are at the limit of our present diagnostic capability. It is essential to include kinetic pressure in full equilibrium reconstructions when performing such stability analysis.

Another topic of interest is determining the cause of the fluctuations seen during our Enhanced $D_\alpha$ regime. In addition to the broadband density fluctuations mentioned in Section III, coherent fast fluctuations, which may be bursting or continuous, are often seen on magnetics diagnostics. These fluctuations, referred to as the 'Fast Edge Mode'[33], have n=1 and m=4 or 5, depending on whether the q=4 or 5 rational surface is located in the pedestal region. They are presumably caused by an edge instability. The peak frequency of 60-90 kHz would imply perpendicular

velocities of $\sim 5 \times 10^4\ m/s$, exceeding the diamagnetic drift velocity even for the steepest estimates of the pressure gradient, which suggests that additional poloidal rotation may be present. Magnetic fluctuations have similar amplitudes ($\sim 5 \times 10^{-5}$) on the high and low field side, indicating that they are not ballooning in nature. The spectra of density and magnetic fluctuations have similar frequency ranges but do not show a statistical correlation. While the Fast Edge Mode does cause small rises in $D_\alpha$ emission, it is not observed in all EDA phases and has occasionally been seen during ELM-free periods. It thus does not appear to be the primary cause of the increased particle transport.

The location of the Fast Edge Mode near a rational surface has led to the investigation of tearing and microtearing modes as possible explanations[28,34]. In a steep pedestal, either the current gradient $j'$ or the temperature gradient $\nabla T_e$ could be destabilizing. When the rational surfaces are located within the pressure pedestal, several radial eigenmodes of the $\nabla T_e$ driven micro-tearing mode have been calculated to become linearly unstable for $L_T = T_e/\nabla T_e \simeq 5$ mm, consistent with the profile shown in Figure 5. Calculations indicate that the m/n=4/1 mode is unstable and that higher m modes can also become unstable as the pedestal approaches the separatrix.

## VI. CONCLUSIONS AND FUTURE PLANS

Measurements to date of the pedestal region on C-Mod, using an extensive diagnostic set, have shown the existence of a steep transport barrier in both temperature and density in H-Mode. The parameters at the top of this barrier cover a wide operational space ($T_e$=150–750 eV, $n_e = 0.5 - 3.3 \times 10^{20}\,\mathrm{m}^{-3}$), depending on the global plasma parameters, input and radiated powers and H-mode regime. Type III ELMs are only seen for $T_e(\psi = 0.95)$ below 200 eV at 5.4 T and 350 eV at 8 T. ELM-free H modes have the highest pedestal temperatures, but tend to be transient. Steady-state Enhanced $D_\alpha$ H-modes generally have slightly lower pedestals in $T_e$, but can have comparable pedestal pressures since they occur at high density.

Edge density profiles are observed by both the reflectometer and Langmuir probes to steepen in H-mode. The $n_e$ barrier width is $\leq 1$ cm, within our diagnostic resolution. $T_e$ pedestal profiles show a barrier width $\Delta_T \simeq$8 mm , again close to the diagnostic resolution. Soft x-ray profiles show even narrower profiles, with $\Delta$ =2–4 mm. The sources of x-ray radiation are not yet determined, but preliminary analysis indicates these profiles would be consistent with $\Delta_T \sim \Delta_n \simeq$3–6 mm. MHD

stability analysis shows that edge currents associated with the pedestal favourably alter the ideal stability boundary, leading to a narrow region which apparently has 'second stable access'. Because of these effects, edge pressure profiles are found to be ideally stable, consistent with the observed absence of Type I ELMs, despite very steep gradients. High frequency fluctuations located in the pedestal region are sometimes observed. Incoherent, broadband density fluctuations increase in the Enhanced $D_\alpha$ H-mode and may be responsible for the increased particle transport. Coherent magnetic fluctuations are sometimes seen, and are associated with rational surfaces within the pedestal. Their high frequency suggests that poloidal rotations may be large.

In future experiments, profile widths will be measured under a wider range of plasma conditions. In particular, it is hoped to establish the scaling with plasma current, magnetic field and density, as well as to compare ELM-free and EDA H-modes. This should help resolve uncertainties about the dependence on $\rho_i$ and $\rho_{i,pol}$ as well as other possible variables such as neutral penetration. The narrow widths measured by the edge soft x-ray array imply that temperature and density profile diagnostics with $\delta R \sim 1$ mm are required to resolve details of the pedestal region. A pedestal Thomson scattering system and heterodyne radiometer are being designed. A diagnostic neutral beam to be installed in 1998 will make possible CXRS measurements of $T_i(R)$ and rotations as well as MSE measurements of current profiles. Other spectroscopic diagnostics are also beginning to measure edge rotations. These quantities will enable us to infer the edge electric field, and should help to give a more complete understanding of the formation and sustainment of the H-mode transport barrier.

**Acknowledgments**

This work was supported by the United States Department of Energy Contract No. DE-AC02-78ET51013. The efforts of the entire C-Mod technical, operations and physics groups in carrying out these experiments are gratefully acknowledged.

## References


[1] ASDEX Team, Nucl. Fusion **29** (11), 1959 (1989).

[2] K. H. Burrell,Phys. Plasmas 4 (5) (1997).

[3] M. Kotschenreuther, W. Dorland, M.A. Beer, G.W. Hammett, Phys. Plasmas **2** (6), 2381, (1995).

[4] I. H. Hutchinson, R. Boivin, F. Bombarda, P. Bonoli, S. Fairfax, C. Fiore, J. Goetz, S. Golovato, R. Granetz, M. Greenwald, S. Horne, A. Hubbard, J. Irby, B. LaBombard, B. Lipschultz, E. Marmar, G. McCracken, M. Porkolab, J. Rice, J. Snipes, Y. Takase, J. Terry, S. Wolfe, C. Christensen, D. Garniew, M. Graf, T. Hsu, T. Luke, M. May, A. Niemczewski, G. Tinios, J. Schachter, J. Urbahn, Phys. Plasmas **1**, 1511 (1994).

[5] M. Greenwald, R. L. Boivin, F. Bombarda, P. T. Bonoli, C. L. Fiore, D. Garnier, J. A. Goetz, S. N. Golovato, M. A. Graf, R. S. Granatz, S. Horne, A. Hubbard. I. H. Hutchinson, J. H. Irby, B. LaBombard, B. Lipschulz, E. S. Marmar, M. J. May, G. M. McCracken, P. O'Shea, J. E. Rice, J. Schachter, J. A. Snipes, P. C. Stek,Y. Takase, J. L. Terry, Y. Wang, R. Watterson, B. Welch, S. M. Wolfe, Nucl. Fusion Vol. 37, No. 6, 793 (1997).

[6] J. L. Luxon, R. Anderson, F. Batty, C. B. Baxi, G. Bramson, N. H. Brooks B. Brown and the DIII-D Team, in *Plasma Physics and Controlled Nuclear Fusion Research, 1986* (International Atomic Energy Agency, Vienna, 1987), Vol. I, 159.

[7] T. H. Osborne, R. J. Groebner, L. L. Lao, A. W. Leonard, R. Maingi, R. L. Miller, G. D. Porter, D. M. Thomas and R. E. Waltz, Proc. 24th EPS Conf. on Controlled Fusion and Plasma Physics, Berchtesgaden, Germany, 1996, (European Physical Society, Petit-Lancy) Vol. 21A, 1101 (1997).

[8] JT-60 Team, in *Proc. 14th Conf. on Plasma Physics and Controlled Nuclear Fusion Research, 1992* (International Atomic Energy Agency, Vienna, 1987), Vol. I, 57.

[9] M. Kikuchi, M. Sato, Y. Koide, N. Asakura, T. Fukuda, S. Ishida, M. Mori, M. Shimada, H. Ninomija, Proc. 20th EPS Conf. on Contr. Fusion and Plasma Physics, Lisboa, 1993, (European Physical Society, Petit-Lancy) Vol. 17C, 179 (1993).

[10] W. Koppendorfer, C. Andelfinger, M. Ballico, and the ASDEX Upgrade and NBI Teams, in *Proc. 14th Conf. on Plasma Physics and Controlled Nuclear Fusion Research, 1992* (International Atomic Energy Agency, Vienna, 1993), Vol. I, 127.

[11] W. Suttrop, O. Gehre, J. C. Fuchs, H. Reimerdes, W. Schneider,J. Schweinzer, ASDEX Upgrade

team, "Effects of Type I Edge Localized Modes on Transport in ASDEX Upgrade", IAEA Technical Committee Meeting on H-modes, Kloster Seeon, Germany, Sept. 1997, submitted to Plasma Phys. and Contr. Fusion.

[12] Y. Takase, R.L. Boivin, F. Bombarda, P.T. Bonoli, C. Christensen, C. Fiore, D. Garnier, J.A. Goetz, S.N. Golovato, R. Granetz, M. Greenwald, S.F. Horne, A. Hubbard, I.H. Hutchinson, J. Irby, B. LaBombard, B. Lipschultz, E. Marmar, M. May, A. Mazurenko, G. McCracken, P. O'Shea, M. Porkolab, J. Reardon, J. Rice, C. Rost, J. Schachter, J.A. Snipes, P. Stek, J. Terry, R. Watterson, B. Welch, S. Wolfe, Phys. Plasmas 4 1647 (1997).

[13] H. Zohm, Plasma Phys. Control. Fusion **38**, 105 (1996).

[14] Y. Takase, R. Boivin, F. Bombarda, P.T. Bonoli, C. Fiore, D. Garnier, J. Goetz, S. Golovato, R. Granetz, M. Greenwald, S.F. Horne, A. Hubbard, I. Hutchinson, J. Irby, B. LaBombard, B. Lipschultz, E. Marmar, M. May, A. Mazurenko, G. McCracken, P. O'Shea, M. Porkolab, J. Reardon, J. Rice, C. Rost, J. Schachter, J.A. Snipes, P. Stek, J. Terry, R. Watterson, B. Welch, S. Wolfe, in Proc. 16th Int. Fusion Energy Conf., Montreal, 1996, (International Atomic Energy Agency, Vienna, 1997), Vol. I, 475.

[15] J.A. Snipes, R.L. Boivin, C. Christensen, D. Garnier, J. Goetz, S.N. Golovato, M. Graf, R.S. Granetz, M. Greenwald, I.H. Hutchinson, J. Irby, B. LaBombard, E.S. Marmar, A. Niemczewski, P.J. O'Shea, M. Porkolab, P. Stek, Y. Takase, J.L. Terry, M. Umansky, S.M. Wolfe, Phys. Plasmas **3**, 1992 (1996).

[16] J.A. Snipes, A.E. Hubbard, D.T. Garnier, S.N. Golovato, R.S. Granetz, M. Greenwald, I.H. Hutchinson, J. Irby, B. LaBombard, E.S. Marmar, A. Niemczewski, P.J. O'Shea, M. Porkolab, P. Stek, Y. Takase, J.L. Terry, R. Watterson, S.M. Wolfe, Plasma Phys. Control. Fusion **38**, 1127 (1996).

[17] A. E. Hubbard, J. A. Goetz, I. H. Hutchinson, Y. In, J. Irby, B. LaBombard, P. J. O'Shea, J. A. Snipes, P. C. Stek, Y. Takase, S. M. Wolfe, Alcator Group, in Proc. 16th Int. Fusion Energy Conf., Montreal, 1996, (International Atomic Energy Agency, Vienna, 1997), Vol. I, 875.

[18] A. E. Hubbard, R. L. Boivin, J. F. Drake, M. Greenwald, Y. In, J. H. Irby, B. N. Rogers and J. A. Snipes,"Local Variables Affecting H-mode Threshold on Alcator C-Mod", IAEA Technical Committee Meeting on H-modes, Kloster Seeon, Germany, Sept. 1997, submitted to Plasma Phys.

and Contr. Fusion.

[19] B. N. Rogers and J. F. Drake, Phys. Rev. Letters **79** 229 (1997).

[20] J. H. Irby, E. S. Marmar, E. Sevillano, S. M. Wolfe, Rev. Sci. Instrum. **59**(8) 1568 (1988).

[21] P. C. Stek, *Reflectometry Measurements on Alcator C-Mod*, PhD thesis, Mass. Inst. of Tech., 1997.

[22] B. LaBombard, J.A. Goetz, I. Hutchinson, D. Jablonski, J. Kesner, C. Kurz, B. Lipschultz, G. M. McCracken, A. Niemczewski, J. Terry, A. Allen, R.L. Boivin, F. Bombarda, P. Bonoli, C. Christensen, C. Fiore, D. Garnier, S. Golovato, R. Granetz, M. Greenwald, S. Horne, A. Hubbard, J. Irby, D. Lo, D. Lumma, E. Marmar, M. May , A. Mazurenko, R. Nachtrieb, H. Ohkawa, P. O'Shea, M. Porkolab, J. Reardon, J. Rice, J. Rost, J. Schachter, J. Snipes, J. Sorci, P. Stek, Y. Takase, Y. Wang, R. Watterson, J. Weaver, B. Welch, S. Wolfe, J. Nucl. Mat. 241-243 (1997) 149.

[23] L.L. Lao, H. St. John, R.D. Stambaugh, A.G. Kellman, W. Pfeiffer, Nucl. Fus. **25** (1985) 1611.

[24] H. Zohm, W. Suttrop, H.J. DeBlank, R.J. Buttery, D. A. Gates, J.A. Heikkinen, W. Herrmann, A. Kallenback, T. Kass, M. Kaufmann, T. Kurki-Sonio, B. Kurzan, M. Maraschek, H. Reimerdes, F. Ryter, H. Salzmann, J. Schweinzer, J. Stober, ASDEX Upgrade, ECRH, ICRH, NBI Teams, in Proc. 16th Int. Fusion Energy Conf., Montreal, 1996, (International Atomic Energy Agency, Vienna, 1997), Vol. I, 439.

[25] G. Janeschitz, A. Hubbard, Y. Igitkhanov, J. Lingertat, T. Osborne, H. D. Pacher, O. P. Pogutse, D.E. Post, M. Shimada, M Sugihara, W. Suttrop, Proc. 24th EPS Conf. on Controlled Fusion and Plasma Physics, Berchtesgaden, Germany, 1996, (European Physical Society, Petit-Lancy) Vol. 21A, 1101 (1997).

[26] J. E. Rice, J. L. Terry, J. A. Goetz, Y. Wang, E. S. Marmar, M. Greenwald, I. Hutchinson, Y. Takase, S. Wolfe, H. Ohkawa, A. Hubbard, Phys. Plasmas **4** (5) 1605 (1997).

[27] P. G. Yushmanov, T. Takizuka, K. Riedel, O. Kardaun, J. Cordey, S. Kaye, D. Post, Nucl. Fusion **30**, 1999 (1990).

[28] J. A. Snipes, R. S. Granetz, M. Greenwald, A. E. Hubbard, I. H. Hutchinson, J. Irby, J. Kesner, S. Migliuolo, T. S. Pedersen, J. Ramos, J. Rice, P. C. Stek, Y. Takase and S. M. Wolfe, "ELMs and fast edge fluctuations in Alcator C-Mod", IAEA Technical Committee Meeting on H-modes, Kloster Seeon, Germany, Sept. 1997, submitted to Plasma Phys. and Contr. Fusion.

[29] R. J. Groebner and T. N. Carlstrom, "Critical Edge Parameters for H-Mode Transition in DIII-D",

IAEA Technical Committee Meeting on H-modes, Kloster Seeon, Germany, Sept. 1997, submitted to Plasma Phys. and Contr. Fusion.

[30] P. H. Rebut, R. J. Bickerton and B. E. Keen, Nucl. Fusion **25** (9), 1011 (1985).

[31] P. Breger, S.J. Davies, C. Flewin, N.C. Hawkes, R.W. T. Konig, V. Parail, Z.A.Pietrzyk, L. Porte, D.D.R. Summers, M.G. von Hellermann, K-D. Zastrow, Proc. 24th EPS Conf. on Controlled Fusion and Plasma Physics, Berchtesgaden, Germany, 1996, (European Physical Society, Petit-Lancy) Vol 21A, 69 (1997).

[32] R.L. Miller,Y.R. Lin-Liu,T.H. Osborne, and T.S. Taylor, "Ballooning mode stability for self-consistent pressure and current profiles at the H-mode edge", IAEA Technical Committee Meeting on H-modes, Kloster Seeon, Germany, Sept. 1997, submitted to Plasma Phys. and Contr. Fusion.

[33] I.H. Hutchinson,R.S. Granetz,A. Hubbard,J.A. Snipes and S.M. Wolfe, Proc. 24th EPS Conf. on Controlled Fusion and Plasma Physics, Berchtesgaden, Germany, 1996, (European Physical Society, Petit-Lancy) Vol. 21A, 557 (1997).

[34] Y.T. Lau, Nucl. Fusion **30** 936 (1990).

**Figure Captions**

FIG. 1. Electron temperature vs density, taken at $\psi = 0.95$, for many C-Mod discharges with $B_T$=5.3-5.45 T and $I_p$=0.78-1.2MA. Open squares indicate time slices in L-Mode, open circles ELM-free H-mode, solid diamonds EDA H-mode and stars H-modes with Type III ELMs. Lower temperature limits for H-mode and upper limits for the presence of ELMs can be seen. An arbitrary constant pressure curve is shown for reference, and does not correspond to a computed stability limit.

FIG. 2. Electron temperature vs density, taken at $\psi = 0.95$, for discharges with $B_T$=7.7-8.0 T and $I_p$=1.0-1.2 MA. The symbols used are the same as in Figure 1.

FIG. 3. Electron density profiles vs normalized radius r/a, measured by reflectometry(cirles) and Thomson scattering (squares), before and after a transition at 0.81 secs from L-mode to ELM-free H-mode, for a discharge with $B_T$=5.4 T and $I_p$=1.0 MA. The L-mode profile (dashed line) is at 0.80 s. The H-mode profile (solid line, 0.82 s) has not yet changed significantly in the core but is already very steep at the edge. The dotted line shows the separatrix position.

FIG. 4. Electron density(top) and temperature(bottom) profiles vs distance from the separatrix, measured by a scanning probe in the SOL in two very similar 800 kA, 5.3 T discharges. The L-mode time slice (dashed curve, 0.72 sec), was just before an L-H transition, with $\overline{n}_e = 2.0 \times 10^{20}\,\mathrm{m}^{-3}$ and $P_{RF} = 0.45$ MW. The H-mode scan (solid curve) was taken at 0.96 s, with $\overline{n}_e = 3.2 \times 10^{20}\,\mathrm{m}^{-3}$ and $P_{RF} = 1.8$ MW, late in an ELM-free H-mode. In both cases the RF power was turned off during the probe scan to avoid possible rectification effects. Both $n_e$ and $T_e$ drop in the scrape-off layer and steepen significantly a few mm outside the separatrix, indicating a transport barrier.

FIG. 5. Edge temperature profile measured using ECE, obtained by ramping the toroidal field from 5.5-5.7 T during the time period 0.72-0.8 seconds on Shot 960206007, a 1 MA H-mode with moderately enhanced $D_\alpha$ emission. The different symbols correspond to different channels of the GPC, which move in time as $B_T$ changes. The dashed curve is a *tanh* fit to the raw data, which gives a width of 12 mm. The thick solid curve is a deconvolved profile taking into account the known radial averaging of the instrument, and gives a width $\Delta_T$= 8 mm.

FIG. 6. Edge radiated power emissivity for discharge 970511024 ($B_T$=5.4T, $I_p$=0.8 MA). The L-mode profile (dashed line) is just before an L-H transition at 0.91 s In the ELM-free H-mode (solid line) the emission drops outside the separatrix and the profile steepens and increases in magnitude. The steep gradient extends at least 1 cm inside the separatrix (the range of the high resolution AXUV diode array).

FIG. 7. Edge x-ray emissivity profiles vs time, again for discharge 970511024. The dashed curve is at 0.91 seconds, before the L-H transition, and shows little emissivity. The solid curves are in H-mode at 0.92 s (+) and 0.96 s (circles), near the end of the ELM-free phase, and show emissivity increasing and developing a steep pedestal, with $\Delta_\varepsilon$ = 3-4 mm. The separatrix is at 89.9 cm.

FIG. 8. Ideal ballooning stability diagram showing $-P'$ vs normalized $\psi$ for Discharge 960227043 at 840 ms, during an Enhanced $D_\alpha$ phase with high edge pressure. The lower set of curves, marked by symbols, show the pressure gradient, $-P'$, input to EFIT. The solid curve (triangles) is for our best estimate of the actual profile, which approximates the the *tanh* profile with $\Delta$ = 8 mm measured in Fig. 5. The stability boundary $P'_{crit}$ shown is by the corresponding (solid) curve; for $\psi \geq 0.98$, $P'$ is unbounded. The dashed curve (diamonds) has a gradient which is 85% higher, corresponding to a profile with only 4.3 mm width. The corresponding 'second stable' region becomes wider, and the profile is still marginally stable. The dotted line (+) is the $P'$ for a profile without a pedestal, extending the core dP/dR to the edge. This gives a nearly flat $P'_{crit}$ (plain dotted line).

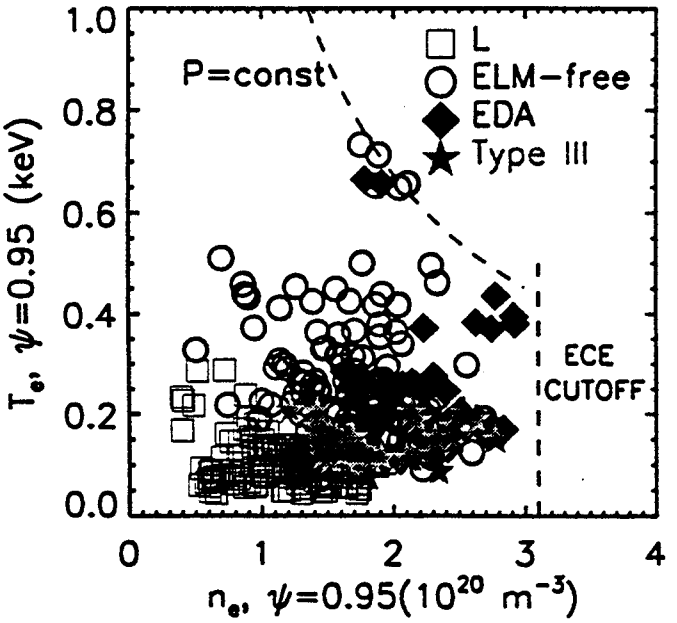


Figure 1

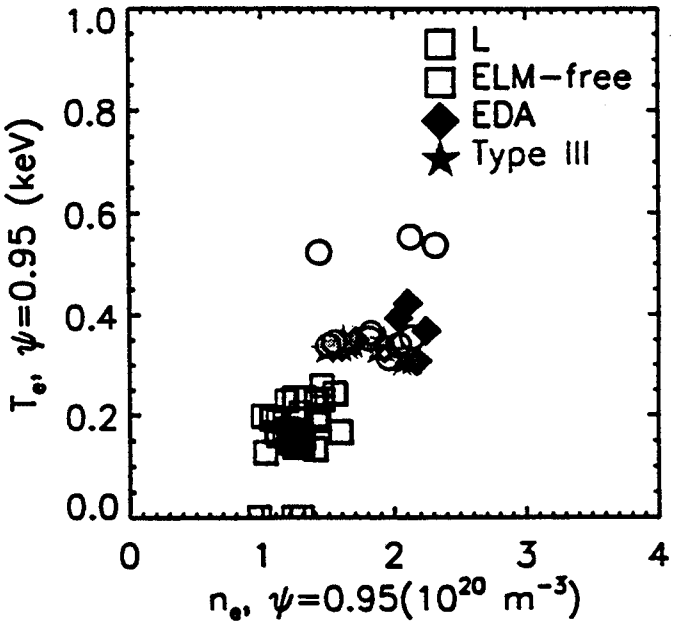


Figure 2

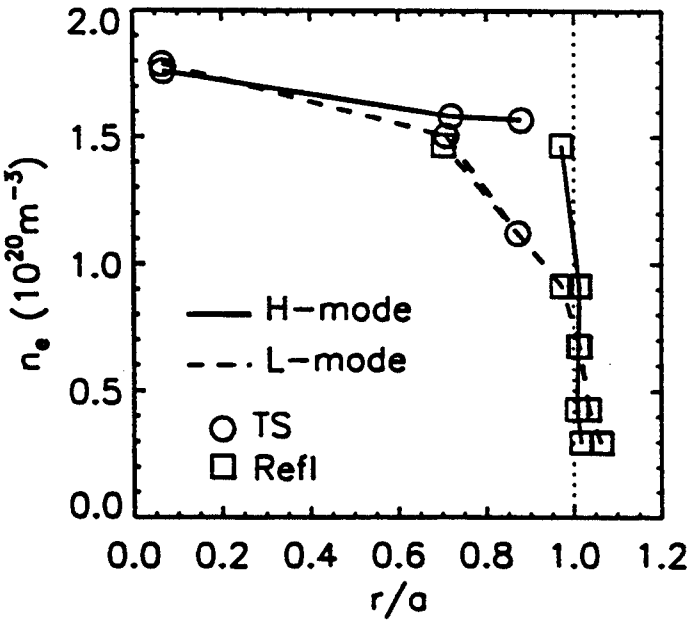


Figure 3

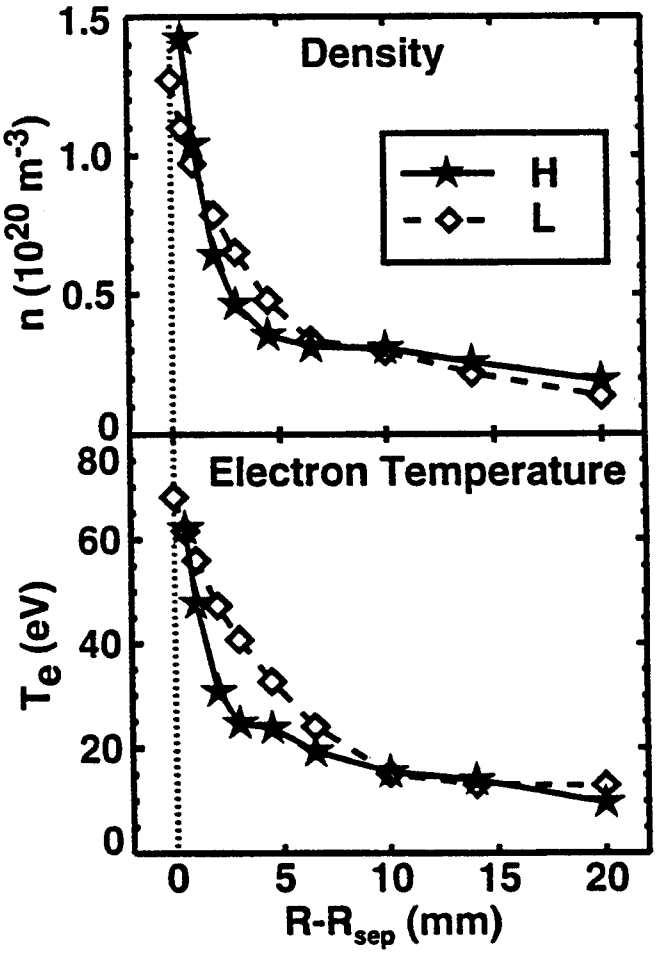


Figure 4

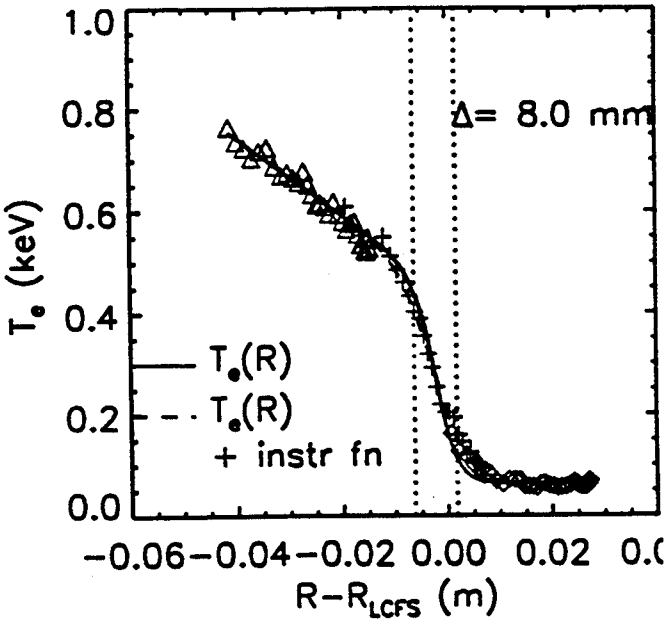


Figure 5

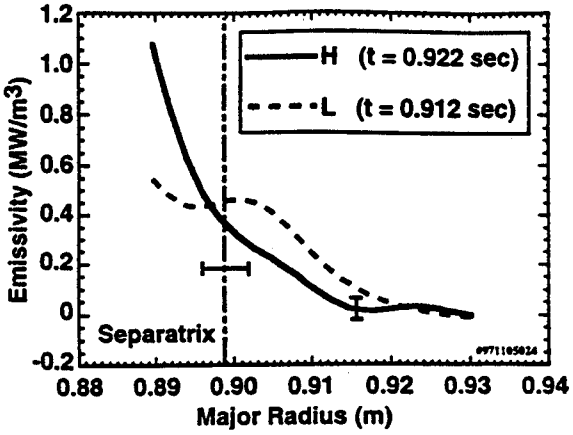


Figure 6

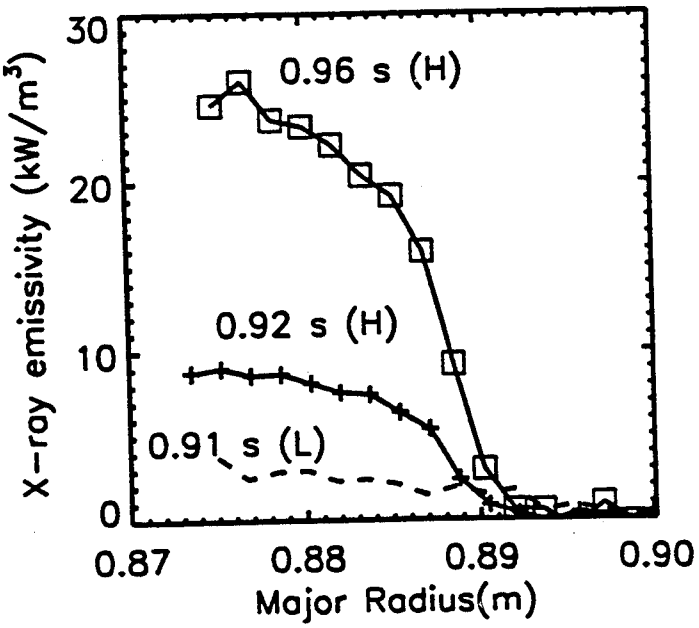


Figure 7

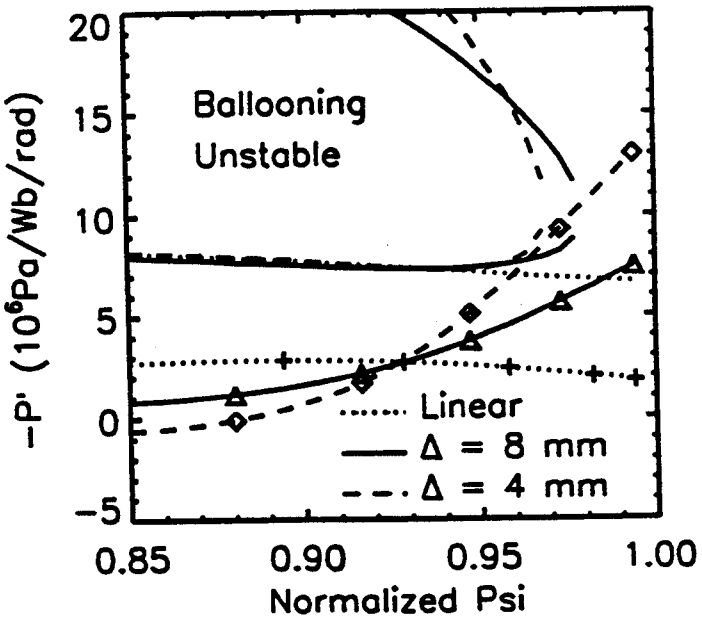


Figure 8